A WIDEBAND PRINTED DIPOLE ANTENNA WITH OPTIMIZED TAPERED FEEDING BALUN FOR ISM AND FWA BANDS

Theodore G. Vasiliadis, Evangelos G. Vaitsopoulos and George D. Sergiadis

Telecommunications Laboratory

Dept. of Electrical and Computer Engineering

Faculty of Engineering

Aristotle University of Thessaloniki

AUTh Campus, GR-54124, Thessaloniki, Greece

tvasilia@auth.gr, sergiadi@auth.gr

Tel. +30-2310-996314

Fax +30-2310-996312

ABSTRACT: This paper presents a wideband printed dipole antenna element. The broad bandwidth is achieved by optimization of the feeding network, which is implemented as a microstrip tapered balun. The design is based on the double-sided flat dipole implementation. The prototype antenna exhibits a measured impedance bandwidth of 58% (VSWR<2), operating over the entire 2.4GHz ISM band and 3.6GHz FWA band.

Keywords: wideband antenna; printed dipole; tapered balun; low-Q antenna; ISM/FWA

1. INTRODUCTION

Modern trends in wireless communications impose the need for design and development of efficient antenna elements, used in products that will eventually operate in contemporary multi-service urban environments, in which several different networks co-exist and interoperate. These antennas are necessary to operate either in a multi-band mode for specific applications or in a wideband mode covering several different services. Moreover, the radiating element has to be compact, for easy integration in devices like computers or PDA's.

Microstrip (printed in general) antennas have been of the most popular types in the past decades, mainly due to their very low profile, low cost of fabrication, easy incorporation into planar arrays, light weight and compatibility with microwave integrated circuit technologies (relatively easy integration in a common PCB with other circuitry). These advantages in most cases were found to outweigh the main electrical disadvantages inherent to this type of radiator, such as narrow bandwidth, spurious feed radiation, poor polarization purity and limited power handling capabilities [1] – [3].

This paper addresses the issue of bandwidth enhancement for a double-sided printed dipole antenna, a microstrip antenna configuration first used by Wilkinson [4]. The printed dipole when compared to the conventional configuration of the microstrip patch antenna, has the advantage of being inherently capable for larger bandwidth [1] as well as occupying less area in the substrate (important in array configurations) [2].

Several different techniques have been proposed in literature, concerning the enhancement of impedance bandwidth in microstrip antennas, mostly by increasing the substrate thickness (this could cause extensive losses in the substrate due to surface wave excitation), by decreasing the substrate dielectric constant, by using parasitic elements (in either stacked or coplanar configurations) and by alternative feeding methods (aperture coupled or proximity feeding instead of direct contacting feed). In most cases, the double-tuning effect is exploited in order to expand the bandwidth [3]. Moreover, in dipole antennas,

increasing the width of the printed arms is identical to increasing the radius of an equivalent wire dipole, which is a well known technique for widening the bandwidth of wire dipoles [5].

Extensive work has been carried out by Levine et al. [6] regarding the effect of dielectric constant and distance of the printed radiator from the ground plane (in suspended plate antennas), where the maximum impedance bandwidth achieved was 25%. By using triangular instead of rectangular dipole arms (bow-tie configuration), the bandwidth can be further expanded to 37% as presented by Bailey [7].

The use of parasitic elements in close proximity to the dipole arms has been proposed by Evtioushkine et al. [8], boosting the initial bandwidth from 39% to an impressive 56% by introducing the parasitic elements, in a suspended over a ground plate configuration. Coplanar parasitic elements have been proposed by Deal et al. [9] in a “quasi-Yagi” configuration, yielding an impedance bandwidth of 48%. A similar Yagi-like double-sided antenna [10], achieved a bandwidth of 37%. Stacked parasitic elements (aperture stacked patches) are widely used for enhanced bandwidth (over an octave), but their fabrication is relatively complicated and expensive.

Single-element antennas without any bandwidth enhancements have been reported in [11] and [12], with bandwidths of 19% and 45% respectively, by simply matching the feeding network to the radiating element. In this paper, we present a wideband double-sided printed dipole antenna, with measured impedance bandwidth of 58%, by optimally selecting the dimensions of the radiator and balun, placing its double-resonance loop at the center of the Smith chart, thus providing high bandwidth without parasitic elements, with minimal design complexity and tolerance to structural parameters.

The operating frequency range of the antenna spans from 2.19 to 3.97GHz (for VSWR<2), thus covering continuously the entire Industrial, Scientific and Medical (ISM) band of 2.4GHz and Fixed Wireless Access (FWA) band of 3.4-3.8GHz. Supported services include the popular Bluetooth and WLAN (IEEE 802.11b/g) protocols, potential WLLs (wireless local loops) based on FWA, as well as other applications like ENG/OB (electronic news gathering/outside broadcasting) video links or radiolocation services.

2. ANTENNA DESIGN AND SIMULATION

The antenna design is based on the double-sided flat dipole implementation [4, 6]. The proposed optimization process includes the design of a balanced radiator (flat dipole) and a stage of designing an optimized balun for this type of radiator. The balun will match the unbalanced coaxial connector feed to the balanced radiator and its behavior is crucial for the final antenna characteristics. Optimum performance is achieved by conducting a parametric study on each design stage.

The proposed antenna geometry is depicted in Figure 1, along with all main design parameters and coordinate axes. The flat dipole is formed by two rectangular strips L=50mm long and W=10mm wide. These arms are printed on both sides of a thin microwave laminate having a relative permittivity of ε_r = 2.21 and substrate thickness of h=1.58mm (Taconic – TLY5). The dipole is center-fed by a short twin-line of broadside parallel strips as illustrated in Figure 2. The parallel strips are L2=4mm long and W2=2mm wide, and they form a balanced feeding line for the flat radiator. The transition from this balanced twin-line to a coaxial unbalanced feed point is implemented using a linear microstrip taper. A 50Ω impedance SMA end-launch connector is soldered at the feed point.

The tapered balun does not match the actual parallel-strips' impedance to the 50Ω coax input, but instead is designed separately in order to optimize the overall antenna performance. Therefore, a discontinuity between the balun and the parallel-strips is apparent (in general, W3 is different than W2). The unbalanced end of the tapered balun resembles a microstrip line of width Wf (mm) over a finite ground plane of width Ws (mm). In order to approximate an ideal microstrip line the ground plane must be much wider than the metallic strip. In the proposed design, a ratio of Ws/Wf = 7 has been proved to be satisfactory. This microstrip approximated line has a 50Ω impedance when Wf = 4.9mm.

Early implementations of the tapered balun [4, 6] suggested that the length of the transition should be gradual for at least a wavelength. In our proposed design, the overall length depends on the opening angle of the strip, equal to a=6°, yielding a taper length of

approximately 14.75mm, which is much smaller than a wavelength. The performance of the taper is adequate for this design, while maintaining a minimal size, which is important for the compact nature of the radiator. The overall laminate area occupied by the antenna is approximately 50x29mm^2.

The electrical properties of the radiating element were simulated using the FDTD method. The values for the aforementioned design parameters were selected from a parametric study (for optimum performance of the final antenna design) and are indicated in Table 1, along with a short description.

Table 1. Design parameters for optimum antenna performance (final design).

Parameter	Value (mm)	Description
L	50	overall dipole length
W	10	dipole strip width
L2	4	parallel-strips' length
W2	2	parallel-strips' width
W3	8	balanced taper's end width
Wf	4.9	unbalanced taper's end width (50Ω)
Ws	34.3	ground plane width (7x Wf)
a	6°	taper's opening angle

The overall length of the dipole arms is defined by the resonant frequency of the antenna. Due to the fact that dielectric substrate covers only a finite region around the dipole (while the rest of the surrounding area is air), the resonant length does not scale inversely proportional to the square root of ε_r, as expected in a homogeneous dielectric medium [2]. The first parametric study, illustrated in Figure 3, shows that the resonant dipole length is approximately 0.42-0.45λ_o (where λ_o is the free space wavelength), for the reason explained above. Figure 3 shows the return loss of the balanced radiating element (without the tapered balun) for various dipole lengths L. The dipole strip width (W) has found to affect significantly the double resonance loop in the impedance locus plot of the balanced radiator. The value W=10mm is chosen in order for the loop to lie on the real impedance axis, as illustrated in Figure 4a.

The resonant frequency is also slightly affected by the width of the parallel strips feed (W2), because this dimension determines the overlap percentage between the two dipole arms. Moreover, this parameter has a major impact on both size and position of the resonance loop, when plotted on a Smith chart, as illustrated in Figure 4b. The length of this twin-line feeder (L2) can be used for optimum placement of the resonance loop according to the desired performance. Appropriate values for the presented antenna design are L2=4mm and W2=2mm.

The impedance of the broadside parallel-strips line of width W2=2mm is approximately 114Ω, based on theory presented in [13, 14]. However, the tapered balun will not match this impedance to the coaxial feed, since generally widths W2 and W3 are different in our proposed design process. Instead, it will act as an impedance transformer between the balanced antenna input impedance and the 50Ω coaxial connector. So far, the selected parameters have yielded an impedance locus as shown in Figure 4b (solid line). With respect to that plot, we have marked the points of zero reactance (resonant frequencies) as (1) 23Ω @ 2.14GHz, (2) 62Ω @ 2.76GHz and (3) 26Ω @ 3.56GHz.

For optimum antenna performance, the balun is expected to act as an impedance transformer from Zin to 50Ω, where Zin is defined by the parallel-strips' width W3 on the balanced taper's end. The tapered transition length will affect the placement of the aforementioned resonance points, resulting to a new set at shifted frequencies. However, it is desirable that the effect of the balun on the impedance locus of the balanced radiator shall not result in size reduction of the resonance loop and, in addition, it shall confine a wide range of frequencies as possible inside the VSWR=2 equivalent circle on the Smith chart.

A final parametric study was conducted in order to extract the balun parameters and overall performance of the dipole antenna. In general, Zin is chosen between the pure resistive impedances of points (1) through (3). If Zin is close to 23Ω or 62Ω then the resonance loop of the final matched antenna will probably extend beyond the constant VSWR=2 circle. The final impedance loci plots for three different parametric cases are illustrated in Figure 5 (solid line represents the performance for the final antenna design).

3. EXPERIMENTAL RESULTS AND MEASUREMENTS

A prototype of the optimized wideband flat dipole antenna was fabricated on a Taconic TLY-5 laminate, based on the dimensions specified in Table 1. All electrical properties and performance were measured using an HP-8720C vector network analyzer. The measured and simulated return loss is plotted in Figure 6. Antenna performance in terms of VSWR is plotted in Figure 7 and finally, the simulated and measured radiation patterns for both E and H-planes are illustrated in Figures 8 through 10, for three different frequencies (2.6, 3 and 3.7GHz respectively).

The prototype antenna exhibits a measured impedance bandwidth of 58%, for a standing wave ratio smaller than 2:1, operating continuously over the entire ISM and FWA bands. The exact operating frequency range is 2.19 – 3.97GHz (VSWR<2). Alternatively, for VSWR<1.5 the dipole antenna yields an impedance bandwidth of approximately 49%, operating between 2.32 – 3.83GHz. For more loose restrictions on impedance bandwidth, namely for VSWR<3, the antenna operates over nearly an octave (2.08 – 4.11GHz).

The radiation characteristics of the proposed antenna are similar to the typical toroid radiation solid, with minor discrepancies compared to the radiated fields of an ideal half-wavelength dipole. Radiation patterns are relative to the absolute antenna gain values, given in Table 2 for each case.

Table 2. Absolute antenna gain (simulated and measured)

Frequency (GHz)	Antenna Gain (dBi)	
	Simulation	Measurement
2.6	2.8	2.9
3	3.8	4.3
3.7	5	5.5

H-plane radiation patterns (azimuth cuts) are approximately omni-directional. However, main radiation is directed towards the negative y-axis (that is, towards the feed), with a back-to-front ratio of about 2-3dB. This effect is mainly caused by the radiated fields of

the feeding balun, which acts as an active part of the dipole radiator in its near vicinity. Moreover, the matching network's tapered ground plane directs a small portion of the radiated energy to azimuth angles off the y-axis, resulting to a slightly asymmetric horizontal radiation pattern.

E-plane radiation patterns (elevation cuts) exhibit the typical nulls on the dipole axis (x-axis), at theta angles 0° and 180°. At the lower frequency range (below 3GHz), elevation patterns present a maximum at angles tilted about 10° above the horizon (y-axis). This effect mainly arises from the fact that double-sided printed dipoles are inherently asymmetric structures, having one arm directly connected to the tapered ground plane of the balun, while the other is connected to the feeding strip.

4. CONCLUSIONS

A wideband flat dipole antenna has been presented in this paper, printed on opposite sides of a thin dielectric laminate. A good agreement has been proved between simulated and experimental results, in terms of S-parameters and VSWR. With the proposed design process, the achieved impedance bandwidth of the prototype antenna was measured at 58%, operating continuously over the frequency range between 2.19 to 3.97GHz, for an acceptable VSWR less than 2:1. The measured radiation patterns are in reasonable agreement with simulated results, approximating the typical dipole behavior with moderate absolute gain and some minor pattern asymmetries.

Enhanced bandwidth is achieved without parasitic elements, only by optimizing the feeding balun, thus providing greater bandwidth while maintaining structural simplicity over previously proposed designs. Additionally, the tapered transition length is less than a wavelength, presenting adequate balun performance while maintaining a compact size. The overall dimensions of the antenna are 50x29mm^2; hence the antenna can be easily integrated in embedded systems or in large planar array configurations. Due to its low-profile and easy fabrication, this element can also be used as a feeder in reflector antennas.

5. REFERENCES

1. K.R. Carver, J.W. Mink, Microstrip antenna technology, IEEE Trans Antennas Propagat, Vol. AP-29, No. 1, (1981), 2-24.

2. D.M. Pozar, Considerations for millimeter wave printed antennas, IEEE Trans Antennas Propagat, Vol. AP-31, No. 5, (1983), 740-747.

3. D.M. Pozar, Microstrip antennas, Proceedings of the IEEE, Vol. 80, No. 1, (1992), 79-91.

4. W.C. Wilkinson, A class of printed circuit antennas, IEEE Antennas and Propagation Society International Symposium Digest, Vol. 12, (1973), 270-273.

5. C.A. Balanis, Antenna Theory – Analysis and Design, 2nd ed., John Wiley & Sons, (1997), 454-456.

6. E. Levine, S. Shtrikman, D. Treves, Double-sided printed arrays with large bandwidth, IEE Proceedings, Vol. 135, Pt. H, No. 1, (1988), 54-59.

7. M.C. Bailey, Broad-band half-wave dipole, IEEE Trans Antennas Propagat, Vol. AP-32, No. 4, (1984), 410-412.

8. G.A. Evtioushkine, J.W. Kim, K.S. Han, Very wideband printed dipole antenna array, Electronics Letters, Vol. 34, No. 24, (1998), 2292-2293.

9. W.R. Deal, N. Kaneda, J. Sor, Y. Qian, T. Itoh, A new quasi-Yagi antenna for planar active antenna arrays, IEEE Trans Microwave Theory and Techniques, Vol. MTT-48, No. 6, (2000), 910-918.

10. G. Zheng, A.A. Kishk, A.B. Yakovlev, A.W. Glisson, Simplified feeding for a modified printed Yagi antenna, IEEE Antennas and Propagation Society International Symposium Digest, Vol. 3, (2003), 934-937.

11. G.Y. Chen, J.S. Sun, A printed dipole antenna with microstrip tapered balun, Microwave Opt Technology Letters, Vol. 40, No. 4, (2004), 344-346.

12. B. Edward, D. Rees, A broadband printed dipole with integrated balun, Microwave Journal, Vol. 30, (May 1987), 339-344.

13. H.A. Wheeler, Transmission-line properties of parallel strips separated by a dielectric sheet, IEEE Trans Microwave Theory and Techniques, Vol. MTT-13, No. 2, (1965), 172-185.

14. B. Bhat, S.K. Koul, Unified approach to solve a class of strip and microstrip-like transmission lines, IEEE Trans Microwave Theory and Techniques, Vol. MTT-30, No. 5, (1982), 679-686.

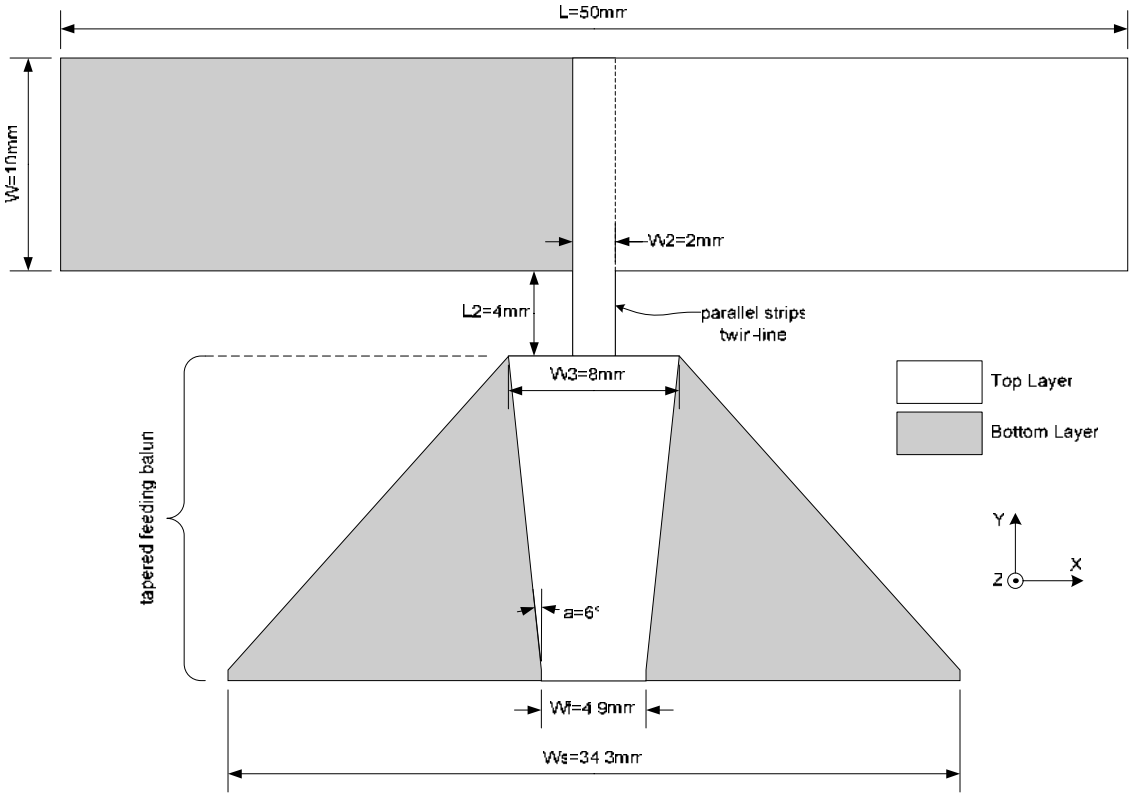

Figure 1. Proposed dipole antenna geometry and parameters, with coordinate axes.

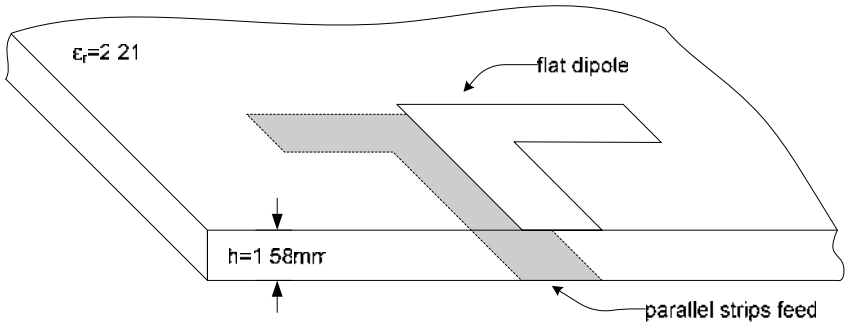

Figure 2. Broadside parallel-strips' feeding line for the flat dipole antenna.

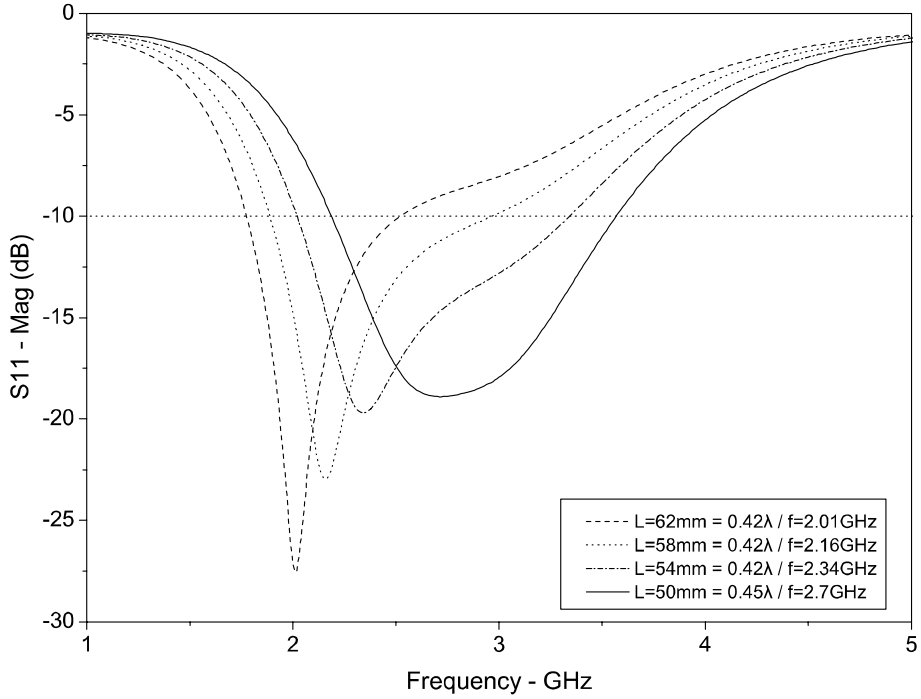

Figure 3. Return loss versus dipole length L for the balanced radiator (without balun) and resonant frequencies (W=10mm, L2=4mm, W2=2mm).

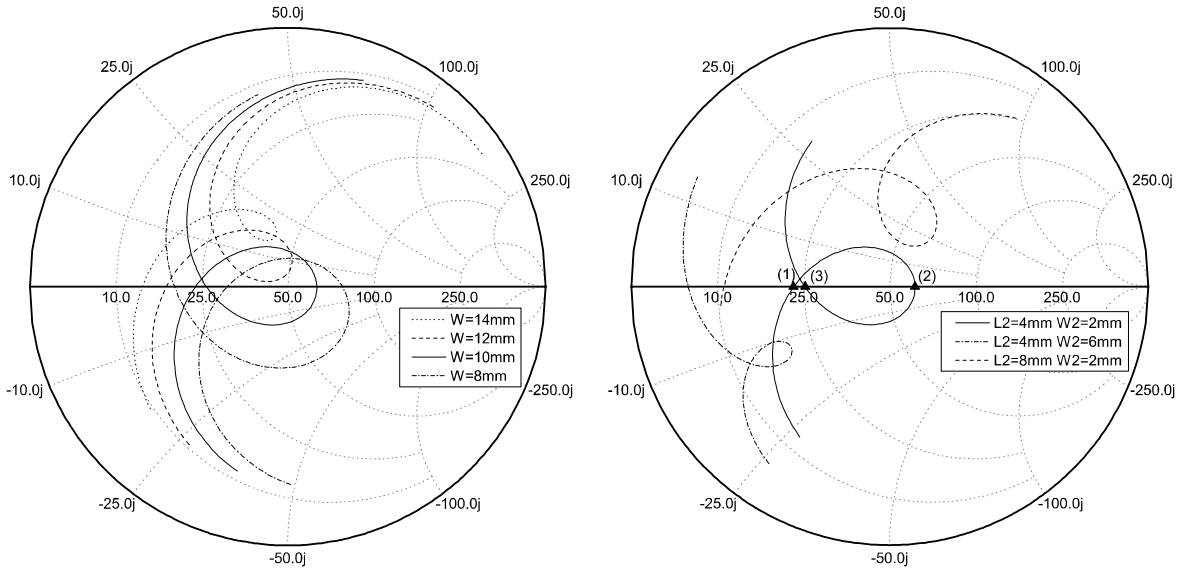

Figure 4. Impedance locus variation on Smith chart for the balanced radiator versus (a) dipole strip width (for L=50mm, L2=4mm and W2=2mm) and (b) parallel strips dimensions L2 and W2 (for W=10mm, L=50mm).

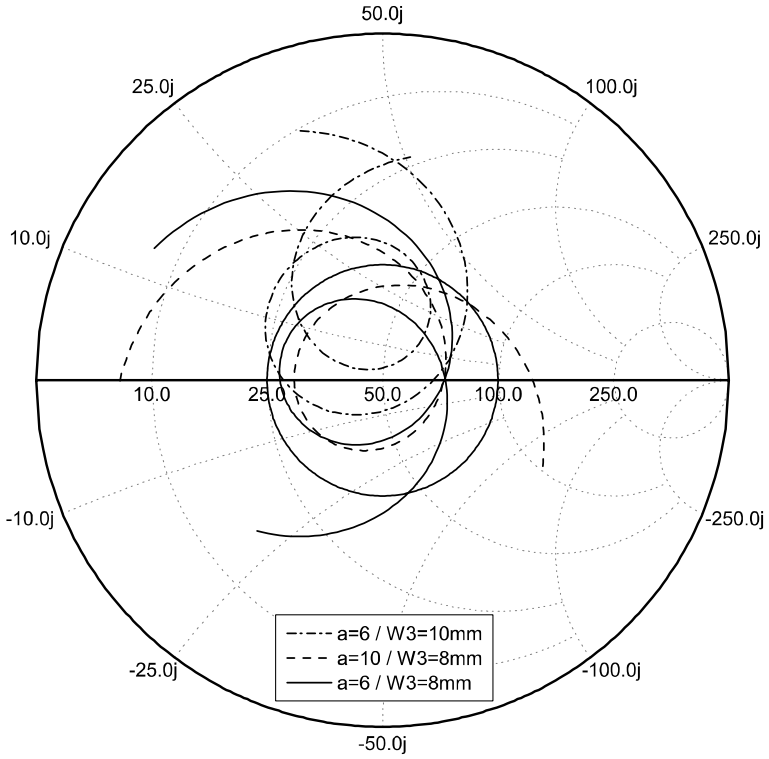

Figure 5. Tapered balun parametric study (for L=50mm, W=10mm, L2=4mm and W2=2mm) and VSWR=2 circle. Solid line represents optimized antenna performance (final design).

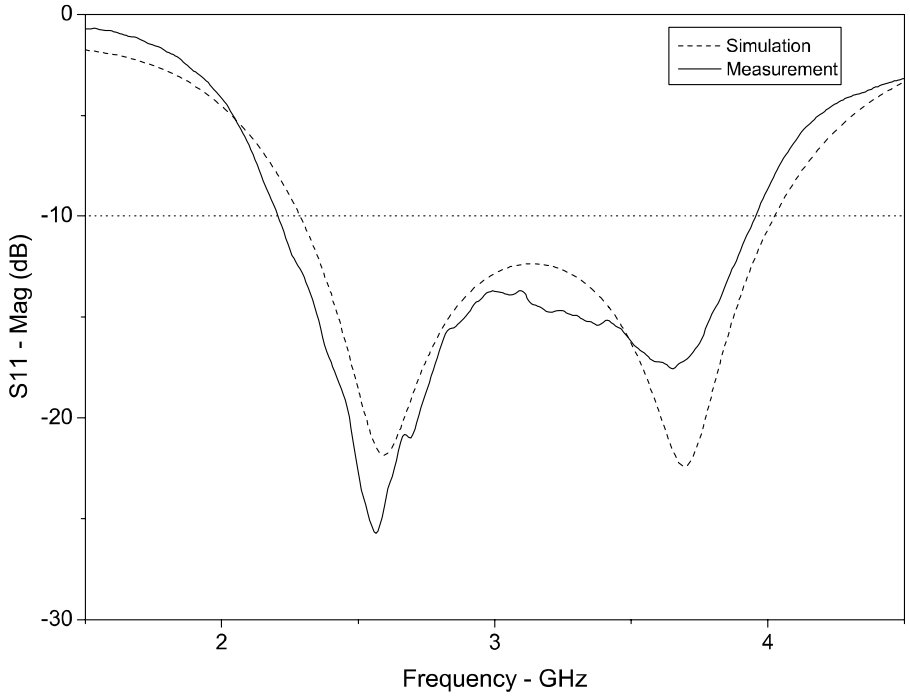

Figure 6. Simulated (dashed line) and measured (solid line) return loss of the prototype antenna.

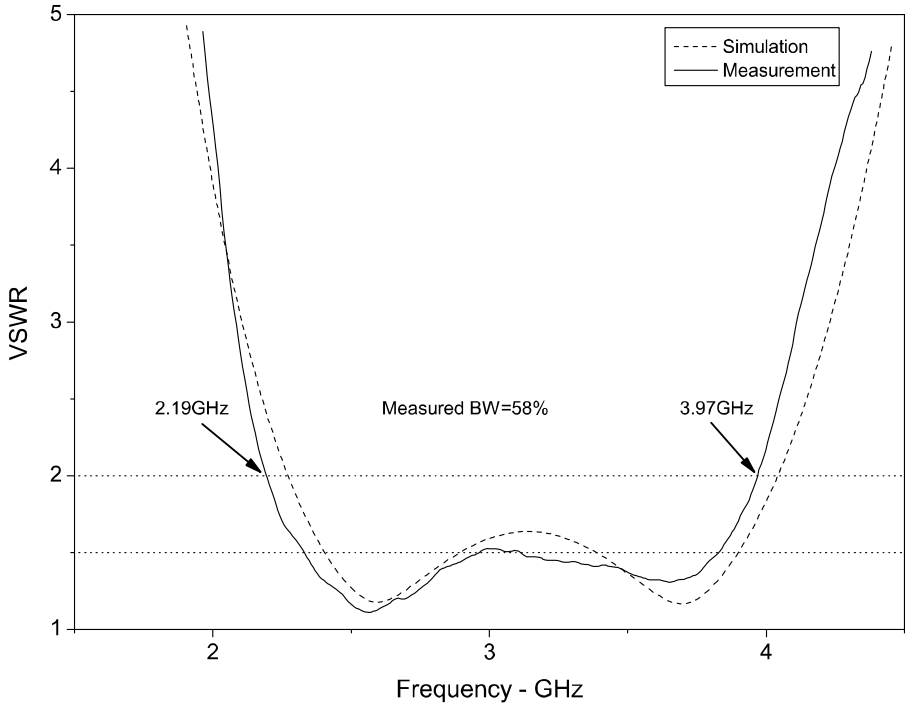

Figure 7. Simulated (dashed line) and measured (solid line) VSWR of the prototype antenna.

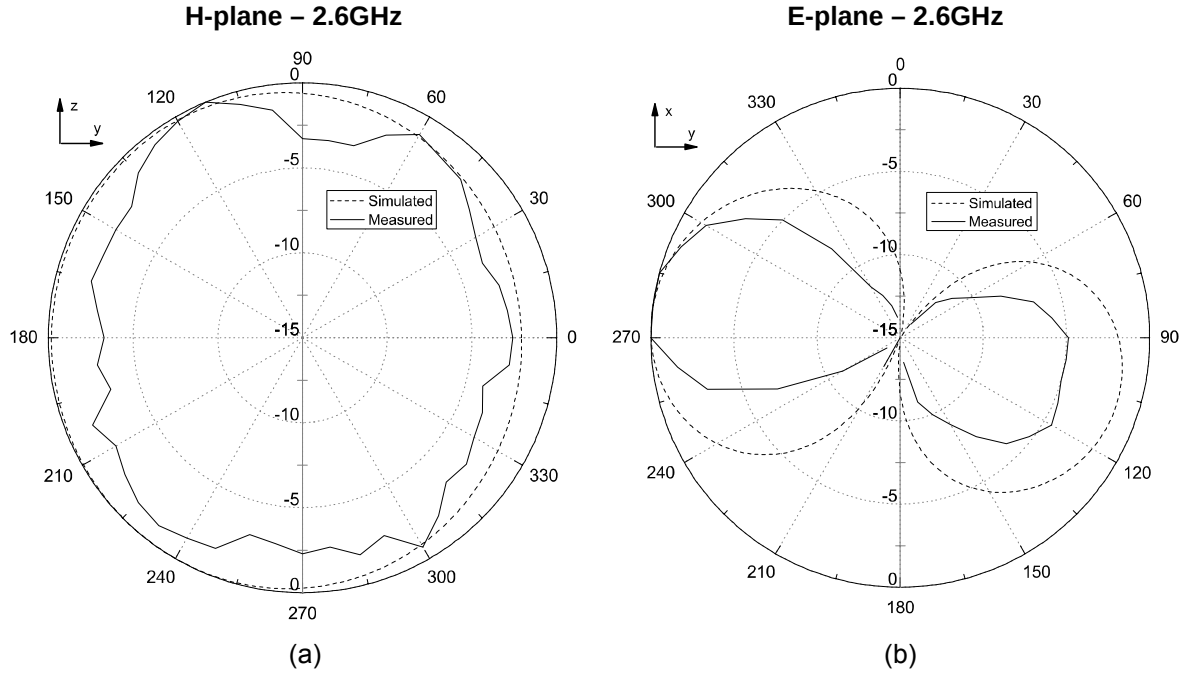

Figure 8. Simulated (dashed) and measured (solid) radiation patterns at 2.6GHz
Absolute gain: 2.8dBi (simulated) / 2.9dBi (measured).

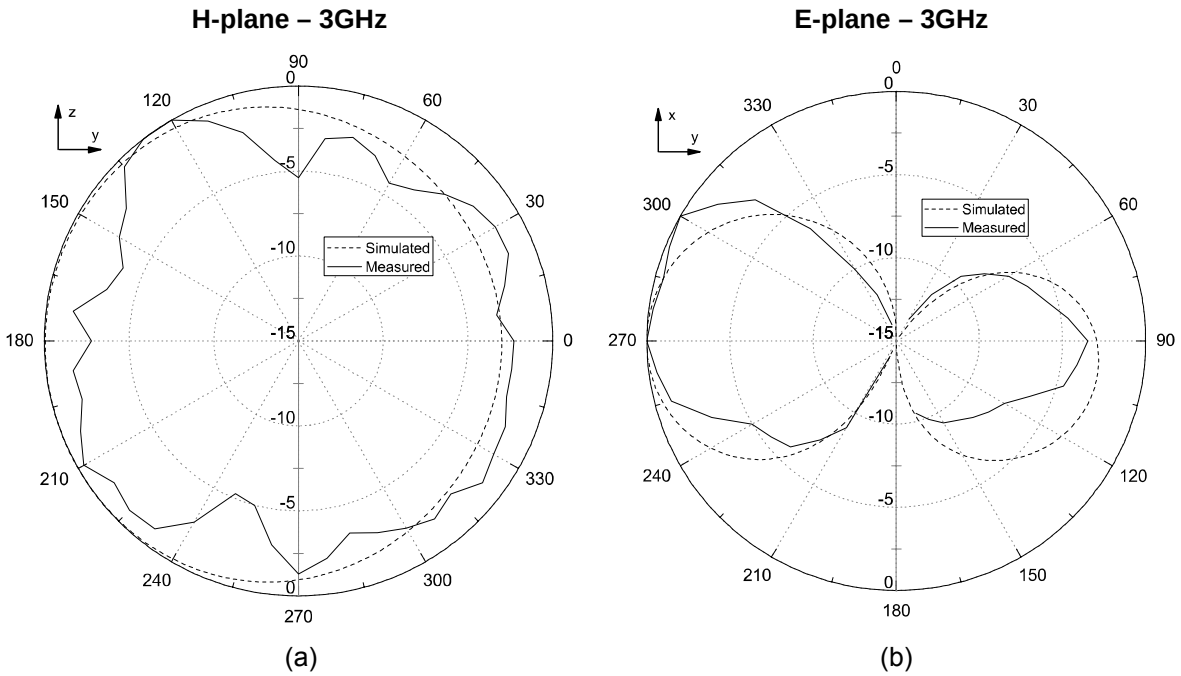

Figure 9. Simulated (dashed) and measured (solid) radiation patterns at 3GHz
Absolute gain: 3.8dBi (simulated) / 4.3dBi (measured).

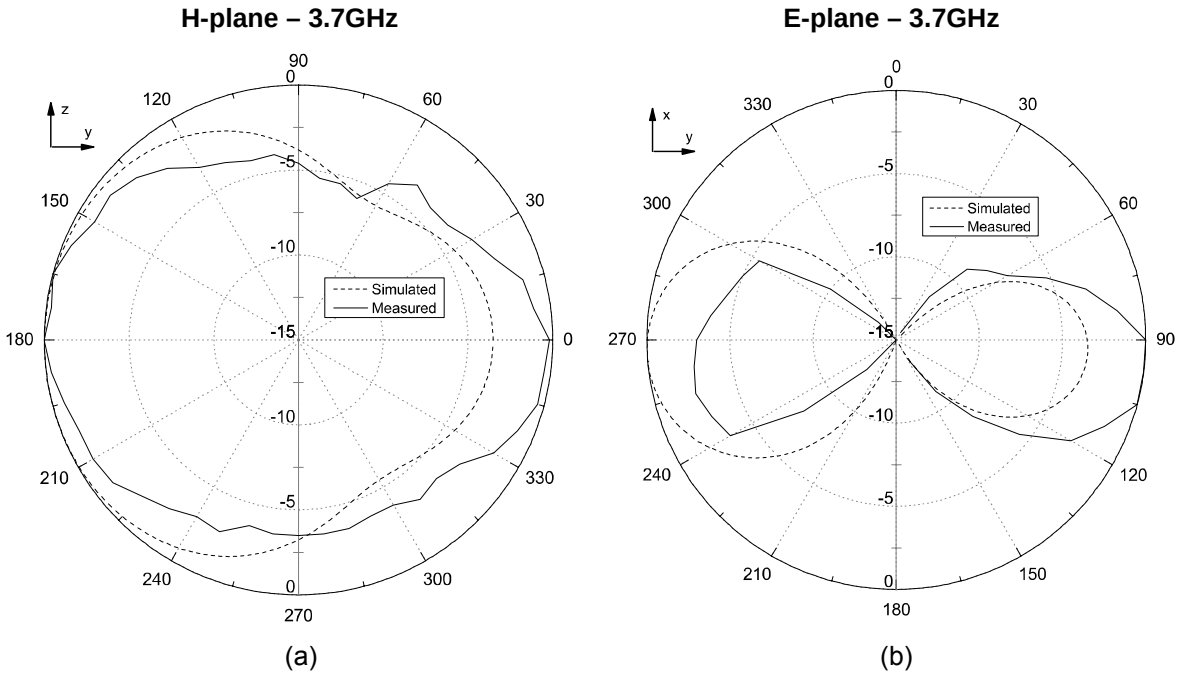

Figure 10. Simulated (dashed) and measured (solid) radiation patterns at 3.7GHz
Absolute gain: 5dBi (simulated) / 5.5dBi (measured).

Figure legends summary

Figure 1. Proposed dipole antenna geometry and parameters, with coordinate axes.

Figure 2. Broadside parallel-strips' feeding line for the flat dipole antenna.

Figure 3. Return loss versus dipole length L for the balanced radiator (without balun) and resonant frequencies (W=10mm, L2=4mm, W2=2mm).

Figure 4. Impedance locus variation on Smith chart for the balanced radiator versus (a) dipole strip width (for L=50mm, L2=4mm and W2=2mm) and (b) parallel strips dimensions L2 and W2 (for W=10mm, L=50mm).

Figure 5. Tapered balun parametric study (for L=50mm, W=10mm, L2=4mm and W2=2mm) and VSWR=2 circle. Solid line represents optimized antenna performance (final design).

Figure 6. Simulated (dashed line) and measured (solid line) return loss of the prototype antenna.

Figure 7. Simulated (dashed line) and measured (solid line) VSWR of the prototype antenna.

Figure 8. Simulated (dashed) and measured (solid) radiation patterns at 2.6GHz Absolute gain: 2.8dBi (simulated) / 2.9dBi (measured).

Figure 9. Simulated (dashed) and measured (solid) radiation patterns at 3GHz Absolute gain: 3.8dBi (simulated) / 4.3dBi (measured).

Figure 10. Simulated (dashed) and measured (solid) radiation patterns at 3.7GHz Absolute gain: 5dBi (simulated) / 5.5dBi (measured).